JOURNAL OF CATALYSIS 125, 488–500 (1990)

Zeolite A-Supported Ru Catalysts

JEFFREY C. S. WU,*,[1] JAMES G. GOODWIN, JR.,*,[2] AND MARK DAVIS†

*Department of Chemical and Petroleum Engineering, University of Pittsburgh, Pittsburgh, Pennsylvania 15261; and †Department of Chemical Engineering, Virginia Polytechnic Institute and State University, Blacksburg, Virginia 24061

Received March 7, 1989; revised June 4, 1990

A series of zeolite A-supported Ru catalysts was investigated to determine the catalytic possibilities when Ru is supported on such small-pore, low Si/Al ratio zeolites. Catalysts prepared by adding a Ru precursor to the zeolite A synthesis gel, designated [ZS], had metal dispersed intrazeolitically, although not uniformly. By comparison, catalysts prepared by surface deposition of Ru on zeolite A, designated [SD], had metal particles primarily on the external surfaces of the zeolite crystallites. All metal sites were accessible for ethane hydrogenolysis; however, molecular sieving strongly influenced cyclopropane hydrogenation. With the exception of the strong molecular sieving effect on the reaction of cyclopropane found for RuNaA[ZS], the most important effect on the catalytic properties was Ru particle size. There was no obvious effect of the method of preparation or the electrostatic field of the zeolite on Ru site activity. The synthesis preparation method was found to offer a viable means for preparing highly dispersed, catalytically active metal particles inside a small-pore zeolite such as A, where other methods are not successful.

I. INTRODUCTION

The advantages of dispersing a catalytic metal within a zeolite pore structure are twofold: high metal dispersion and possible reaction selectivity enhancements due to molecular sieving. Usually, the catalytic metal (e.g., Ru) can easily be introduced into large-pore zeolites (*1*). Although zeolite A is well known structurally (*2*, *3*) and is heavily used for adsorption, there has been little research reported dealing with zeolite A-supported zero-valent metal catalysts, with the exception of that of Fraenkel and Gates (*4*) for a CoA catalyst. Probably this is due in large part to the great difficulty of introducing metals into zeolite A by the standard preparation procedures. However, it has been recently shown that zeolite A-supported metal catalysts can be prepared by adding metal solutions directly to the zeolite A synthesis gel before crystallization (*5*, *6*). As far as can be discerned, there have been no previous studies of small-pore zeolite-supported metal catalysts prepared by such a synthesis technique.

Hydrogenolysis and hydrogenation of hydrocarbons have found wide application for probing the catalytic behavior of supported metals. Ethane hydrogenolysis (*7–13*), especially, has been studied extensively. It is generally accepted that this catalytic reaction is structure-sensitive. Catalytic reaction of cyclopropane over supported metals has also been found to be useful in the characterization of active catalytic centers (*14–23*). It has recently been demonstrated to be also somewhat structure-sensitive (*19*, *20*). The kinetic diameters of ethane (3.8 Å) and cyclopropane (4.2 Å) make them excellent probe reactants for zeolite A-supported metal catalysts. The apparent pore sizes of CaA and

[1] Current address: Alcoa Separations Technology Division, Warrendale, PA.

[2] To whom correspondence should be addressed.

0021-9517/90 $3.00

NaA are 4.4 and 4.0 Å, respectively. Thus, ethane molecules are able to enter the cavities of both zeolites, while cyclopropane molecules are excluded by NaA.

This paper reports the results of a study of the catalytic properties of a series of zeolite A-supported Ru catalyst using, among other things, the two probe reactions cited above.

II. EXPERIMENTAL

Materials

RuNaA[ZS] ("ZS" indicating zeolite synthesis) was prepared by adding $[Ru(NH_3)_5Cl]Cl_2$ solution directly to the zeolite A synthesis gel prior to crystallization. RuCaA[ZS] was prepared from the Na form of the catalyst precursor (RuNaA[ZS]) prior to reduction by cation exchange at room temperature with $CaCl_2$. This exchange did not alter the Ru content within the limit of experimental error in Ru determination, probably because of the difficulty of diffusion of the cationic Ru complex. RuNaA[SD] ("SD" indicating surface deposition) was prepared by contacting an aqueous solution of $RuCl_3$ with NaA zeolite. RuCaA[SD] was prepared from RuNaA[SD] by cation exchange with $CaCl_2$. This was accompanied by a 50% loss of Ru. The detailed preparation procedures are given in the literature (*5*, *6*). All the catalysts were reduced by heating up to 400°C (0.5°C/min) and holding for 4 h in flowing hydrogen.

The Ru metal loadings of the catalysts were determined by atomic absorption. XRD was carried out on all the catalyst samples using CuK_α radiation in order to detect any changes in crystallinity of the zeolite after various stages of preparation and pretreatment.

Transmission electron microscopy (TEM) was used to study the metal location and size. The results are given in Table 1.

TABLE 1

Characteristics of the Catalysts

	Ru[a] (wt%)	Dispersion[b] (%)	d_p[b] (Å)	d_p[c] (Å)
RuNaA[ZS]	0.41	23	39	42
RuCaA[ZS]	0.41	44	20	55
RuNaA[SD]	0.20	30	30	28
RuCaA[SD]	0.10	57	16	<10

[a] Determined by AA with a maximum error of 10% of the measured value.

[b] Estimated by hydrogen chemisorption.

[c] Surface-area mean diameter estimated by TEM.

Hydrogen Chemisorption

Hydrogen chemisorption results were used to determine the metal dispersion and average metal particle size of all the catalysts. H_2 chemisorption measurements were carried out in a standard static gas volumetry system with an attainable vacuum of 10^{-6} Torr. Each catalyst sample was heated from room temperature to 400°C (2°C/min) under vacuum. When the temperature reached 400°C, H_2 (250–300 Torr) was introduced to reduce the catalyst for 1 h at 400°C. After reduction, the cell was evacuated at 400°C for 1 h to desorb hydrogen. The catalyst was then cooled to room temperature under vacuum.

The measurement of H_2 chemisorption was carried out at room temperature. The amount of strongly chemisorbed hydrogen on a Ru catalyst was calculated by extrapolating the total and reversible isotherms to zero pressure and taking the difference. The calculation of metal dispersion was based on $H/Ru_S = 1$.

Ethane Hydrogenolysis

Ethane hydrogenolysis was carried out at 1 atm pressure in a quartz tubular microreactor with a 3/8-in. (1 in. = 2.54 cm) inside diameter. The prereduced catalyst (50 mg) was loaded into the reactor and rereduced under flowing H_2 by ramping the temperature from ambient to 400°C (2°C/min) and holding it there for 2 h. The temperature was then lowered to the desired reaction temperature. Ultrahigh-purity hydrogen and helium and CP-grade ethane (Linde Co.)

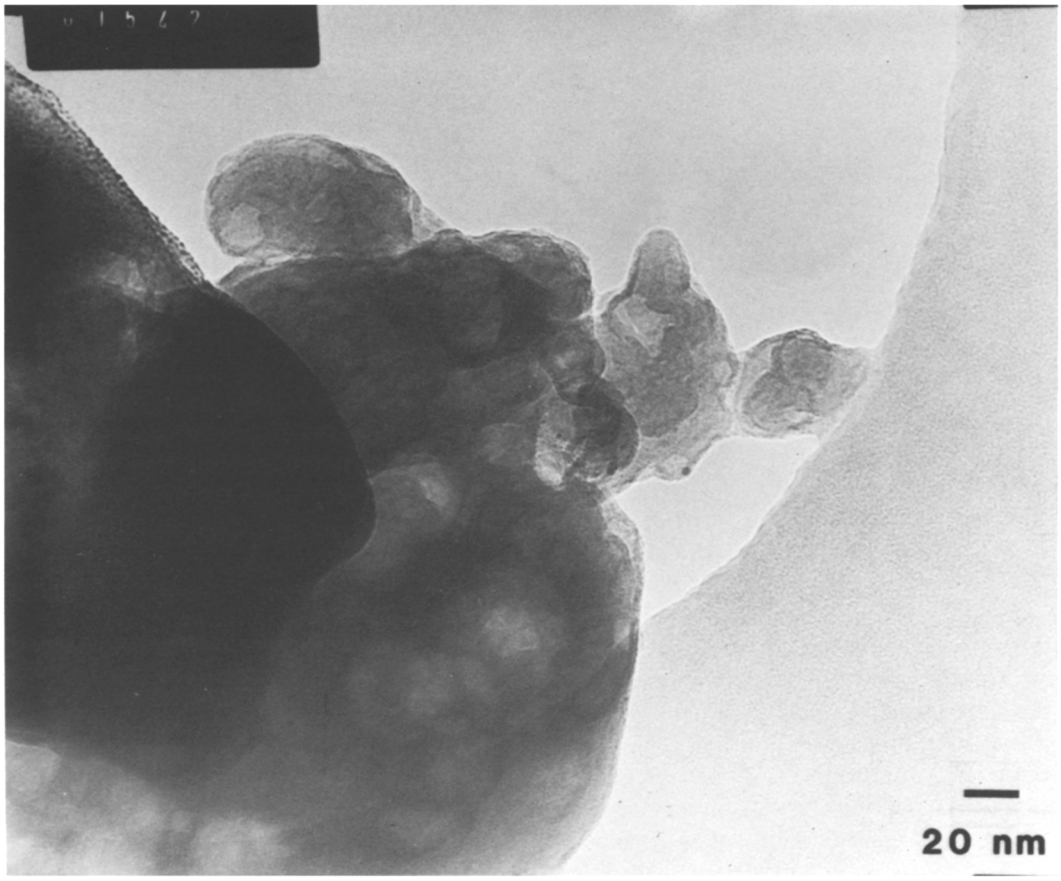

FIG. 1. TEM micrograph of RuNaA[SD].

were used. The flow rate of the reaction mixture, which contained 1.5% ethane, 20% hydrogen, and 78.5% helium, was 100 ml/min.

The reaction was carried out for 3 min at a time. Hydrogen bracketing, at the next reaction temperature, was used for about 15 min between each reaction period. The reaction was first carried out at 250°C and then at several different temperatures (in the range 175°C–270°C) in order to permit a determination of the apparent activation energy. Finally, the reaction was carried out again at 250°C to check for any change due to deactivation during the reaction study. The H_2 bracketing used was found to prevent any significant overall deactivation of the catalysts during the reaction study. The composition of the effluent gas was analyzed by on-line gas chromatography using an 80/100 Porapak Q column.

Cyclopropane Hydrogenation

The reactor, reduction procedures, product analysis, and reactant mixture were the same as those used for ethane hydrogenolysis except that the 1.5% ethane was replaced by 1.5% cyclopropane (CP grade, Linde Co.).

The catalyst (50 mg) was mixed with an equal weight of SiO_2 to minimize the temperature gradients due to the exothermic reaction. RuCaA[ZS] was so active that only 11 mg (mixed with 89 mg of SiO_2) was used in order to keep the conversion low. Conver-

sion was kept lower than 5%. The initial two reaction segments were carried out in 1 and 2 min in order to observe the adsorption of cyclopropane. Each following reaction period lasted 3 min. Hydrogen bracketing, which was at the next reaction temperature, was used between each reaction period for approximately 30 min. This was sufficient to maintain the catalysts' activities. The reaction temperature was varied between 46 and 18°C.

In order to observe cyclopropane adsorption by the zeolites A in the absence of reaction on the metal sites, runs were carried out under the same conditions as those used for cyclopropane reaction using 50 mg of NaA or CaA without any Ru. These molecular sieves (obtained from Aldrich) were dried at 90°C for 18 h and then pretreated with flowing hydrogen in a manner identical to that with the Ru catalysts prior to the adsorption measurements.

III. RESULTS

X-ray diffraction results did not indicate any detectable changes in the zeolite structure as a result of catalyst preparation and pretreatment.

Figures 1–4 show typical TEM micrographs of the catalysts. Defect structures consisting of approximately spherical void spaces (diameters from 100 to 600 Å) observed in the zeolite supports were due to

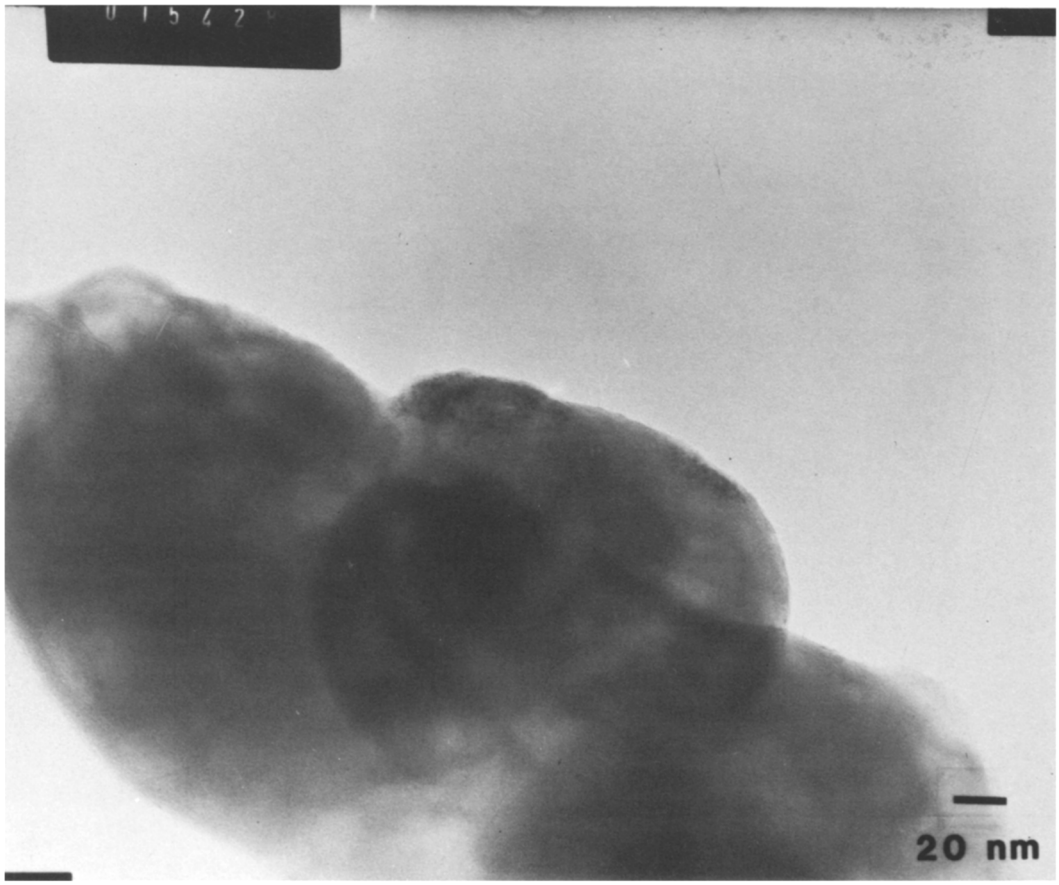

FIG. 2. TEM micrograph of RuCaA[SD].

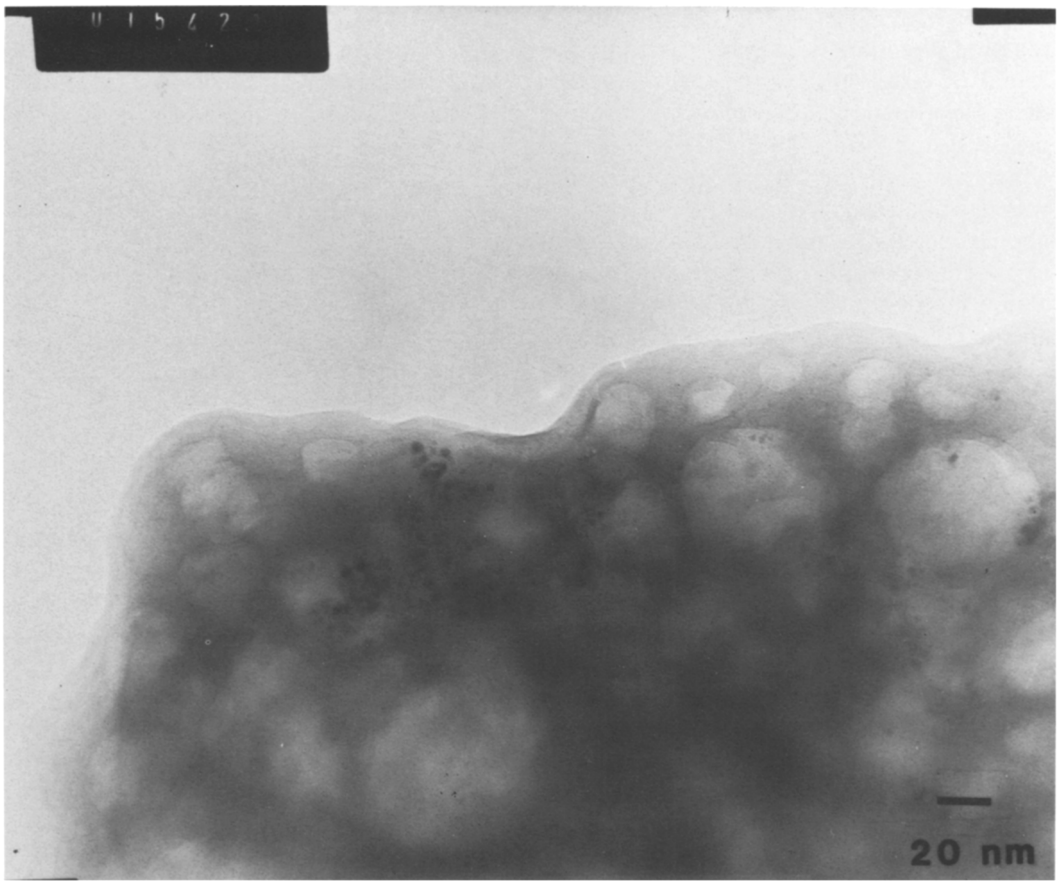

FIG. 3. TEM micrograph of RuNaA[ZS].

electron beam damage in the TEM (*26*). This susceptibility to beam damage is due to the high Al content and lower thermal stability of zeolite A. The beam damage did not appear to affect the metal crystallite sizes seen (*26*). For RuCaA[SD], most metal particles appeared to be under 10 Å and thus were not able to be accurately measured due to the resolution of the TEM (about 10 Å). The surface-area means of the metal particle diameters, based on TEM measurements and the assumption of spherical particles, are listed in Table 1. The metal dispersion and average metal particle diameter determined by hydrogen chemisorption are also listed for comparison. The average metal particle diameters from H_2 chemisorption were calculated using Eq. (1) from Boudart and Djega-Mariadassou (*24*):

$$d_p \text{ (in Å)} = [9.0/(\%D)] \times 100. \quad (1)$$

Table 2 gives the results for ethane hydrogenolysis (Eq. (2)) at 200°C.

$$C_2H_6 + H_2 \rightarrow 2\ CH_4 \quad (2)$$

Arrhenius plots for this reaction are given in Fig. 5. TOFs for the reaction of both ethane and cyclopropane are based on the amount of irreversible hydrogen chemisorption.

Table 3 provides the results for cyclopropane reaction at 20°C. The apparent activa-

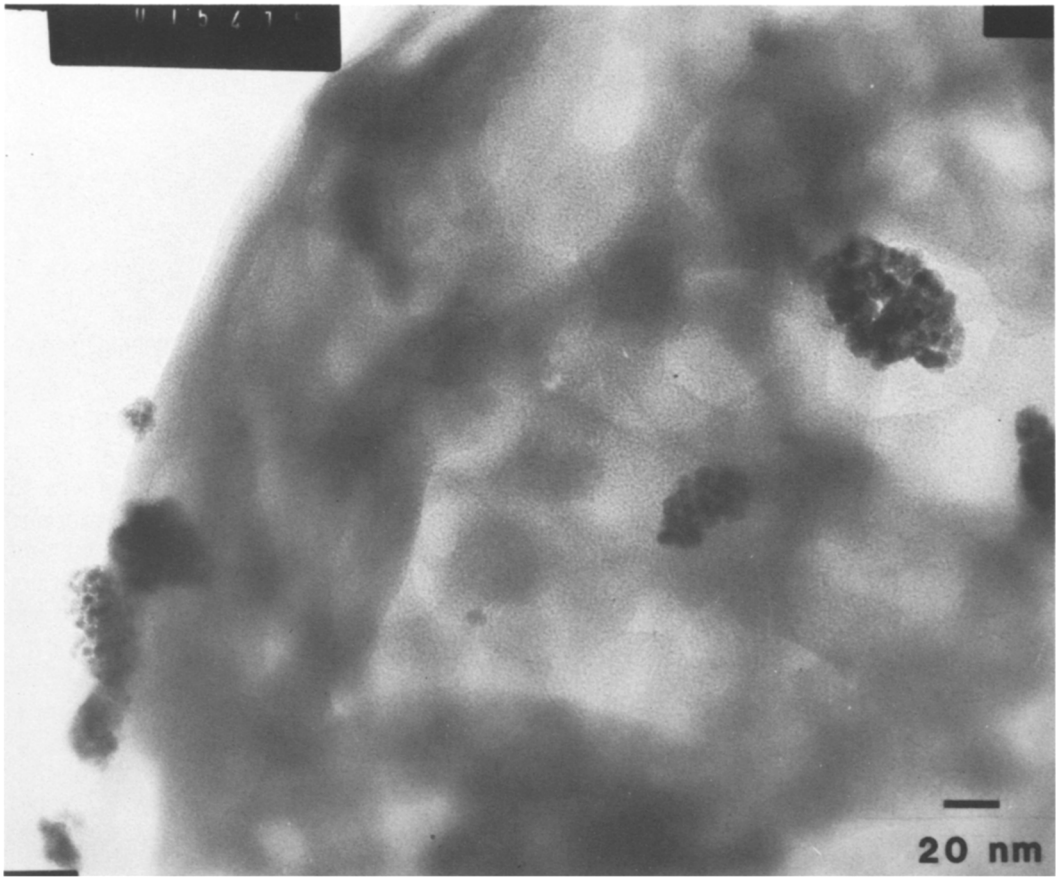

FIG. 4. TEM micrograph of RuCaA[ZS].

tion energies of cyclopropane reaction were determined from the Arrhenius plots (Fig. 6). The activity of RuNaA[ZS] for cyclopropane hydrogenation was so low that no products were detected (>1 ppm) within the entire temperature range 18–46°C). There are three possible reactions in cyclopropane hydrogenation. Reaction 1 (Eq. (3)) is called

TABLE 2
Ethane Hydrogenolysis at 200°C

	Conversion[a] (%)	TOF[b] (1/sec) ×1000	Temp range (°C)	E_a (kJ/mole)
RuNaA[ZS]	0.89	21.1	175–250	100 ± 5
RuCaA[ZS]	2.53	30.0	175–250	111 ± 3
RuNaA[SD]	0.55	19.0	175–250	131 ± 6
RuCaA[SD]	0.09	3.2	200–270	97 ± 8

[a] Based on product formation rate after 6 min of reaction at 200°C.
[b] TOF at 200°C based on H_2 chemisorption.

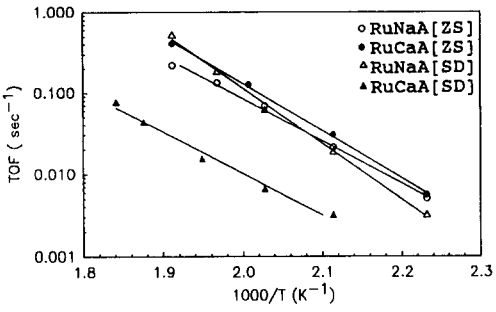

FIG. 5. Arrhenius plots for ethane hydrogenolysis.

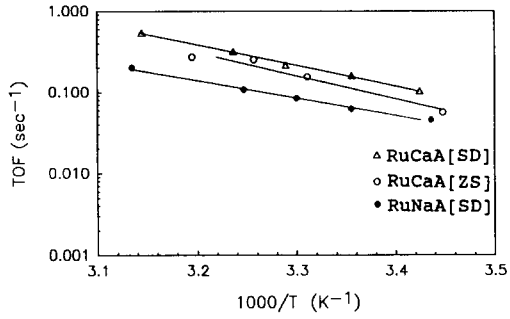

FIG. 6. Arrhenius plots for cyclopropane hydrogenation.

ring opening or hydrogenation; reaction 2 (Eq. (4)) is called hydrogenolysis or selective hydrocracking; and reaction 3 (Eq. (5)) is called nonselective hydrocracking.

Reaction 1 $c\text{-}C_3H_6 + H_2 \rightarrow C_3H_8$ (3)

Reaction 2 $c\text{-}C_3H_6 + 2\,H_2 \rightarrow CH_4 + C_2H_6$ (4)

Reaction 3 $c\text{-}C_3H_6 + 3\,H_2 \rightarrow 3\,CH_4$ (5)

Nonselective hydrocracking was not observed for any of the catalysts since the methane/ethane molar ratio of products was always close to 1. Most of the cyclopropane reaction was contributed by hydrogenation (90%+). Although the TOFs in Table 3 and Fig. 6 are for the combination of reactions 1 and 2, we hereafter use the term "hydrogenation" to denote the reaction.

Because the initial adsorption of cyclopropane by the CaA-form catalysts was so significant, the adsorption of cyclopropane was measured on A zeolites without any Ru for comparison. Figure 7 gives the net adsorption rate of cyclopropane at room temperature by NaA and CaA as well as by the supported metal catalysts. A blank test using the empty reactor permitted measurement of the time lag between the reactor and the GC. The results show that cyclopropane was adsorbed by CaA but not significantly by NaA. These data were obtained by sampling the effluent mixture after various periods of cyclopropane flow. Hydrogen bracketing for 15 min was used between measurements to desorb any adsorbed cyclopropane. This was found to be sufficient. The net adsorption rate was calculated by

TABLE 3

Cyclopropane Hydrogenation at 20°C

	Conversion[a] (%)	TOF[b] (1/sec) ×1000	Temp. range (°C)	E_a (kJ/mole)
RuNaA[ZS]	BDL	BDL	18–46	—
RuCaA[ZS]	1.6	82	17–40	54 ± 10
RuNaA[SD]	1.5	50	18–46	41 ± 2
RuCaA[SD]	3.1	113	19–45	49 ± 2

Note. BDL, below detection limit. Catalyst charge: 50 mg, except RuCaA[ZS] was 11 mg.

[a] Based on product formation rate after 6 min of reaction at 20°C.

[b] TOF for reaction at 20°C based on H_2 chemisorption.

$$\text{Net ads. rate} = \frac{(\text{moles of carbon in/min}) - (\text{moles of carbon out/min})}{3} \quad (6)$$

The results for NaA and CaA without Ru in the flowing cyclopropane mixture also showed that no cyclopropane hydrogenation or selective hydrocracking occurred on the zeolites at the reaction temperatures used for this study.

Figure 7 shows that, after 3 min of cyclopropane flow, the net adsorption rate approached zero. Thus, the adsorption of cyclopropane by the zeolite did not skew the analysis of reaction products after 3 min of flow. To ensure that the reactions were stabilized and to avoid errors due to initial cyclopropane uptake by the zeolite, reaction data were considered only after a total of 6 min of initial reaction and each additional reaction period was set for 3 min, followed by 30 min of hydrogen bracketing.

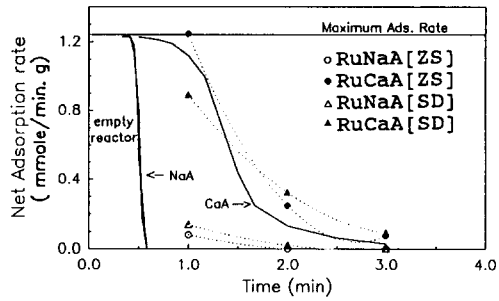

FIG. 7. Adsorption of cyclopropane at 20°C.

IV. DISCUSSION

Metal Particle Size and Location

For RuNaA[SD], and RuCaA[SD], TEM micrographs (Fig. 1 and 2) show that most of the metal particles were on or near the exterior surface of the zeolite crystallites. Shannon *et al.* (*1*) were not successful in dispersing Rd intrazeolitically when preparing RhNaA by ion exchange using $RhCl_3$. They assumed that $Rh(OH)_3$ was perhaps precipitated on the exterior of the NaA crystallites. Na zeolites in aqueous media are known to result in a slightly basic solution (ca. pH of 8). In addition, zeolite surfaces can initiate hydrolytic processes. While the chemistry of Ru in solution is quite complex, it can be suggested that the presence of Na^+ cations in the solution, aided perhaps by the zeolite surface, resulted in the formation of insoluble $Ru_2O_3 \cdot nH_2O$ from $RuCl_3$ (*30, 31*). Such hydrous oxides are known to sometimes become colloidal (*31*). In any case, large molecules such as these would be unable to penetrate through the cage opening of zeolite A, thereby excluding preparation of highly dispersed metal catalysts. Salts such as $Ru(NH_3)_6Cl_3$ are typically used to prepare ion-exchanged zeolite-supported Ru catalysts due to their ability to maintain (at acidic pH's) Ru cations in solution. However, such salts give Ru cations too large to exchange with interior sites in small-pore zeolites like A, thus excluding their use in preparing highly dispersed Ru catalysts.

In RuNaA[ZS] and RuCaA[ZS], it appears that clusters of metal particles were located primarily inside the zeolite crystallites or surrounded by zeolitic material (Fig. 3 and 4). This becomes even more evident later after discussion of the cyclopropane reaction results for RuNaA[ZS].

Table 1 shows the average metal particle diameters calculated by TEM and by H_2 chemisorption. Since H_2 chemisorption is a nondiscriminatory surface technique, the estimated metal particle diameter is an average. In the TEM micrographs, metal particles under 10 Å were not counted due to resolution limitations (about 10 Å). This portion of the particles could contribute significantly to overall H_2 chemisorption. By and large, the agreement between average Ru particle diameters estimated using TEM and chemisorption is excellent. The exception is that for RuCaA[ZS]. Probably the difference observed for this catalyst is due to an overestimation of particle sizes from the TEM micrographs due to the clustering and close proximity of many particles (Fig. 4), resulting in difficulty in separating one particle from a group of several. Thus, the

average particle size calculated from hydrogen chemisorption should be considered in this case to better represent the true structure of the catalyst. Although hydrogen chemisorption in this case provides a better measurement of the number of metal atoms exposed, the accuracy of any secondary calculation (percentage dispersion and average metal particle size) is obviously dependent on an accurate measurement of metal loading, decidedly tricky for such low loadings as found here. However, the by-and-large excellent agreement in average metal crystallite size by TEM and hydrogen chemisorption provides a confirmation that the metal loadings determined were reasonably accurate.

The average metal particle sizes of Ru NaA[ZS] and RuCaA[ZS] are larger than the diameter (11.4 Å) of the α-cages in zeolite A. Since zeolite A possesses a straight pore system, it is possible that metal particles could have been connected through the 8-member ring window (*25*). Also, a few large metal particles could perhaps have existed on the external surface of the zeolite crystallites. However, given the cyclopropane reaction results for RuNaA[ZS] discussed below, it is most likely that large Ru particles (>12 Å) were able to form at defect sites/holes *inside the zeolite crystallites*.

Ethane Hydrogenolysis

The kinetic diameter of ethane (3.8 Å) is smaller than the aperture of A zeolites and, therefore, ethane can enter the zeolite cavities without any hindrance. Thus, there should have been no molecular sieving during ethane hydrogenolysis even for different cation forms of the Ru/A catalysts. Consequently, metal sites in the zeolite A catalysts should have been equally accessible to ethane molecules whether the metal was inside the cavities or on the external surface of the zeolite crystallites. The apparent activation energies (97–131 kJ/mole) are almost the same within experimental error and are well within the range of values, 88–171 kJ/mole, reported in the literature (*9*). In addition, the Arrhenius plots (Fig. 5) of the rates show no curvature, again suggesting no significant diffusion control during reaction in this temperature range.

Figure 5 and Table 2 show that the TOFs for ethane hydrogenolysis on the Ru/A catalysts were similar except for those obtained on RuCaA[SD]. The relative variation in TOF with average particle size between 20 and 40 Å is comparable to that seen for Rh by Yates and Sinfelt (*12*). Ethane hydrogenolysis is well known to be a strongly structure-sensitive reaction. Yates and Sinfelt (*12*) reported that, for ethane hydrogenolysis, the specific catalytic activity of silica-supported Rh increased as particle size decreased. However, for low loadings of Rh (<0.3 wt%) with extremely high dispersions, the specific activity was lower than that which would have been predicted by extrapolation of the higher Rh loading results. These results make sense in light of those for ethane hydrogenolysis on single crystal planes of Ni (*28*) and on supported Ni (*29*). For Ni, the less dense (100)-plane is much more active than the more dense (111)-plane. The higher activity on the less dense plane has been suggested by Goodman (*28*) to be due to the fact that ethane cannot adsorb without breaking the C–C bond. Since there is an increase in concentration of less dense planes as metal crystallite size decreases below 100 Å, one would expect TOF to increase with a decrease in particle size. However, since ethane hydrogenolysis requires as many as 12 surface metal atoms (*29*), the overall TOF would drop for a very highly dispersed system because of the lack of suitable ensembles. This may in part be due to the metal particle sizes and in part due to the increased difficulty of reducing completely very highly dispersed metals. A similar overall increase in TOF of ethane hydrogenolysis with decrease in metal particle size as seen for Rh has also been seen for Ru (*19*). The wt% of Ru and the average metal particle size of Ru

CaA[SD] (<10 Å, Table 1) was much less than that of the other catalysts (all greater than 20 Å according to H_2 chemisorption and TEM) and, hence, that catalyst exhibited a significantly lower TOF than the other catalysts for the reasons discussed above.

Since the TOF results are easily explained by the particle size and loading effects, there was apparently no significant effect on ethane hydrogenolysis due to differences in preparation or support (Ca or Na forms).

Cyclopropane Hydrogenation

The kinetic diameter of a cyclopropane molecule is about 4.2 Å (*2*) which is close to the 4.0 to 4.4 Å apparent pore size of A zeolites. In a dehydrated A zeolite, 8 Na^+ are displaced 0.4 Å into the α-cage from the center of the 6-member ring (Na_I). Three Na^+ are located in the 8-member ring displaced about 1.2 Å from the center (Na_{II}). The Na_{II} cations, by partially blocking the aperture, regulate the pore size and influence the adsorption of molecules. The remaining Na cations, Na_{III}, have been located opposite the 4-member rings. When exchanged by Ca^{2+} so that there are 4 Ca^{2+} and 4 Na^+ in each unit cell, the 8 site I positions are occupied and the site II positions are vacant. Consequently, the apertures are completely open and capable of admitting molecules with kinetic diameters of 4.4 Å or less (*2*).

Theoretically, cyclopropane molecules are able to enter the cavities of zeolite A. However, because of hindrance by the neutralizing cations in NaA, cyclopropane cannot easily penetrate the narrow pores (*15*). Figure 7 shows that significant amounts of cyclopropane can be adsorbed by CaA. This indicates that cyclopropane molecules are able to enter CaA and remain there. For NaA, the net adsorption curve is almost equal to that of the empty reactor, suggesting that cyclopropane molecules are excluded from entering the NaA zeolite crystallites.

Since RuNaA[ZS] was inactive for cyclopropane reaction but was very active for ethane hydrogenolysis, it may be concluded that most of the Ru particles were intrazeolitic and could not be reached by cyclopropane molecules due to Na^+ hindrance of their diffusion. For RuNaA[SD] and Ru CaA[SD], Ru particles were apparently located on the external zeolite surface and, consequently, equally accessible on both catalysts. Thus, whether or not cyclopropane could penetrate into the pores did not affect their TOFs. As can be seen in Fig. 6, the TOFs of RuCaA[ZS] fall between those of RuNaA[SD] and RuCaA[SD]. The difference in TOFs between these catalysts, as discussed later, can be explained by a metal particle size effect.

The amount of cyclopropane adsorption in CaA at these temperatures and this partial pressure of cyclopropane was found to be about 1.217 mmole/g by integrating the area under the CaA adsorption curve and subtracting the area under the empty reactor curve in Fig. 7. This amount of cyclopropane would occupy approximately 20% of the void volume of CaA if the adsorbed cyclopropane were in a condensed phase (liquid). Even though reaction temperatures were well above the boiling point of cyclopropane(−34°C), it is quite possible that so much cyclopropane was able to be adsorbed due to capillary condensation and chemisorption. The average concentration in the zeolite pores is estimated to have been about 3.3 mole/liter. In addition to cyclopropane, the cavities would have contained H_2 and the product molecules. It is possible that any liquid-phase cyclopropane fills only those cavities without Ru sites, the pores in the neighborhood of the Ru sites being kept open by the generation of gaseous products. Thus, the concentration of cyclopropane around the active metal sites would have been much lower than the estimated average concentration, and no effect of cyclopropane concentration would be seen for Ru CaA[ZS] compared to the surface-deposited catalysts. The lack of such a cyclopropane

concentration effect when one considers the effect of Ru particle size is seen later.

Galvagno *et al.* (*17*) and Dalla Betta *et al.* (*23*) reported an apparent activation energy for cyclopropane hydrogenation on Ru/SiO_2 of about 50 kJ/mole. Wallace and Hayes (*21*) found that the apparent activation energy on a Ru sponge was 46 kJ/mole. Table 3 shows that the apparent activation energies of the three active catalysts are similar in value to those in the literature. Thus, an effect of diffusion resistance on cyclopropane hydrogenation can be ruled out for these catalysts. This is not surprising for Ru/A catalysts prepared by surface deposition since the metal sites were predominately on the exterior of the zeolite. Considering the activity of the catalysts and the kinetic diameter of cyclopropane (4.2 Å) relative to the aperture of CaA (4.4 Å), however, it might be surprising that RuCaA[ZS] did not exhibit diffusion control. For RuCaA[ZS], which was prepared from RuNaA[ZS] and which also probably had mainly intrazeolitic Ru particles, cyclopropane molecules were apparently able to enter the cavities and diffuse rapidly to where the metal sites were located. That most of the Ru sites in RuCaA[ZS] had to be readily accessible for cyclopropane reaction is evident from the reasonable value of the TOF. The effective diffusivity of cyclopropane in CaA would have had to be $>10^{-8}$ cm^2/sec in order to avoid mass transfer limitation under the reaction conditions used. This value falls within the accepted range for configurational diffusion.

Recent reports have shown that cyclopropane hydrogenation is somewhat structure-sensitive on supported Ru catalysts where the smaller the metal particle size, the higher the TOF (*19*, *20*). Wong *et al.* (*22*) also observed a metal particle size effect for cyclopropane hydrogenation on Rh/SiO_2 catalysts. The TOFs of the Ru/A catalysts are similar to the TOFs of the catalysts studied by Schwank and co-workers (*19*, *20*), where Ru dispersion was between 20 and 60%. Table 1 shows that Ru/A catalysts had average metal particle sizes as determined by H_2 chemisorption in the order RuNaA[SD] > RuCaA[ZS] > RuCaA[SD]. Thus, barring any support effects, the TOFs of these catalysts would be expected to be in the order RuCaA[SD] > RuCaA[ZS] > RuNaA[SD]. The results in Table 3 verify this prediction.

One of the factors which could influence cyclopropane hydrogenation is the neutralizing cations (*14*, *15*). Although the polarizing power of the neutralizing cations in large-pore zeolites (e.g., X or Y zeolites) may not be significant (*19*), it could be an important factor which might influence the catalytic activity in small-pore, low Si/Al ratio zeolites, such as A. The reason is not only that the interaction distance of cations in A zeolites is small (cage diameter = 11.4 Å for the α-cage) but also that the concentration of neutralizing cations is high (due to Si/Al = 1.0–1.2). Thus the electrostatic field in A zeolites could have a notable influence on an absorbed molecule, especially one as highly strained as cyclopropane. Since most metal sites of RuCaA[ZS] were inside the zeolite crystallites, the neutralizing cations would have had more of an influence on reaction on that catalyst than on the other catalysts. There are no indications, however, to lead one to conclude that such a cation effect played any role in the activity of RuCaA[ZS], especially since the known particle size effect can explain so completely all the results. Taking into account this particle size effect, the catalytic properties of RuCaA[ZS] for cyclopropane hydrogenation on a per Ru surface atom basis appear to be identical to those of Ru CaA[SD] and RuNaA[SD].

V. CONCLUSIONS

Zeolite A-supported Ru catalysts prepared by adding the metal salt directly to the zeolite synthesis gel resulted in the formation of clusters of intrazeolitic metal particles. Those prepared by surface deposition

had metal particles scattered on the surface of the zeolite crystallites. TEM showed that each catalyst had its own metal particle distribution pattern. By and large, average particle sizes from TEM were consistent with those from H_2 chemisorption.

Metal particle size played an important role in ethane hydrogenolysis and cyclopropane hydrogenation. All metal sites on the different catalysts were equally accessible for ethane hydrogenolysis. Difference in TOFs was concluded to be due solely to particle size effects. Molecular sieving, however, was able to exhibit a strong influence on cyclopropane hydrogenation. While the apparent activation energies for cyclopropane hydrogenation of RuNaA[SD], Ru CaA[SD], and RuCaA[ZS] suggest no mass transport limitations, the cyclopropane was essentially blocked from entering RuNaA[ZS]. This caused RuNaA[ZS] to have negligible activity. These results can easily be explained by the fact that cyclopropane can diffuse relatively easily into CaA while for all intents and purposes it is excluded from NaA due to the smaller pore opening. RuNaA[SD] had reasonable activity since most if not all of the Ru particles existed on the external zeolite surfaces.

The electrostatic field of the zeolite did not apparently play any role in the reaction of cyclopropane on the Ru sites inside the RuCaA[ZS] catalyst. This result suggests that such electrostatic fields as exist in zeolite pore systems are not strong enough to affect the ring opening of a molecule even as strained as cyclopropane.

The results of this study point out the utility of using structure-sensitive reactions and the reaction of different size molecules to characterize the average size and location of metal particles in small-pore zeolites.

ACKNOWLEDGMENTS

The authors thank Mr. John Schott of the University of Pittsburgh Applied Research Center for taking the TEM micrographs and assisting in the interpretation of the results. Funding for this study was from the Exxon Educational Foundation.

REFERENCES

1. Shannon, R. D., Vedrine, J. C., Naccache, C., and Lefebvre, F., *J. Catal.* **88,** 431 (1984).
2. Breck, D. W., "Zeolite Molecular Sieves, Structure, Chemistry, and Use," p. 83, Wiley, New York, 1974.
3. Howell, P. A., *Acta. Crystallogr.* **13,** 737 (1960).
4. Fraenkel, D., and Gates, B. C., *J. Amer. Chem. Soc.* **102** (7), 2478 (1980).
5. Rossin, J. A., and Davis, M. E., *J. Chem. Soc., Chem. Commun.*, 234 (1986).
6. Davis, M. E., Saldarriaga, C., and Rossin, J. A., *J. Catal.* **103,** 520 (1987).
7. Bond, G. C., and Hierl, G., *J.Catal.* **61,** 348 (1980).
8. Camilleri, P., Marshall, R. M., and Purnell, J. H., *J. Chem. Soc., Faraday Trans. 1* **70,** 1434 (1974).
9. Galvango, S., Schwank, J., Gubitosa, G., and Tauszik, G. R., *J. Chem. Soc., Faraday Trans. 1* **78,** 2509 (1982).
10. Rouco, A. J., and Haller, G. L., *J. Catal.* **72,** 246 (1981).
11. Rouco, A. J., Haller, G. L., Oliver, J. A., and Kemball, C., *J. Catal.* **84,** 297(1983).
12. Yates, D. J. C., and Sinfelt, J. H., *J. Catal.* **8,** 348 (1967).
13. Sàrakàny, A., Matusek, K. and Tètènyi, P., *J. Chem. Soc., Faraday Trans. 1* **73,** 1699 (1977).
14. Förster, H., and Seebode, J., *Zeolites* **3,** 63 (1983).
15. Fejes, P., Kiricsi, I., Förster, H., and Seebode, J., *Zeolites* **4,** 259 (1984).
16. Beaumont, R., Ha, B., and Barthomeuf, D., *J. Catal.* **40,** 160 (1975).
17. Galvagno, S., Schwank, J., and Parravano, G., *J. Catal.* **61,** 223 (1980).
18. Kiricsi, I., Hannus, I, Varca, K., and Fejes, P., *J. Catal.* **63,** 501 (1980).
19. Sajkowski, D. J., Lee, J. Y., Schwank, J., Tian, Y, and Goodwin, J. G., Jr., *J. Catal.* **97,** 549 (1986).
20. Schwank, J., Lee, T. Y., and Goodwin, J. G., Jr., *J. Catal.* **108,** 495 (1987).
21. Wallace, H. F., and Hayes, K. E., *J. Catal.* **29,** 83 (1973).
22. Wong, T. C., Brown, L. F., and Haller, G. L., *J. Chem. Soc., Faraday Trans. 1* **71,** 519 (1981).
23. Dalla Betta, R. A., Cusumano, J. A., and Sinfelt, J. H., *J. Catal.* **19,** 343 (1970).
24. Boudart, M., and Djega-Mariadassou, G., "Kinetics of Heterogeneous Catalytic Reactions," p. 26, Princeton Univ. Press, Princeton, NJ, (1984).
25. Gustafson, B. L., and Lunsford, J. K., *J. Catal.* **74,** 393 (1982).

26. Davis, M., unpublished results.
27. Chen, Y. W., Wang, H. T., and Goodwin, J. G., Jr., *J. Catal.* **83,** 415 (1983).
28. Goodman, D. W., "Eighth International Congr. Catal.," Berlin, 1984.
29. Martin, G. A., *Catal. Rev. Sci. Eng.* **30,** 519 (1988).
30. Charonnat, R., *in* "Nouveau Traité de Chimie Minérale," Vol. 19, p. 117, Masson et Cie., Ed., Paris, 1958.
31. Cotton, F. A., and Wilkinson, G., "Advanced Inorganic Chemistry," 3rd ed., p. 1007, Interscience, New York, 1972.